SUPPLEMENTAL MATERIAL

Supplemental Methods

Reagents and Antibodies

Synthetic LXR ligand 3-[3-[N-(2-Chloro-3-trifluoromethylbenzyl)-(2,2-diphenylethyl)amino]propyloxy]phenylacetic acid hydrochloride (GW3965) was kindly donated by Jon Collins (GlaxoSmithKline, Research Triangle Park, NC). Natural LXR ligand 22(*R*)-hydroxycholesterol [22(*R*)-HC], 2,3,5-triphenyltetrazolium chloride (TTC), and 4',6-diamidino-2-phenylindole (DAPI) were purchased from Sigma-Aldrich (St. Louis, MO). Dihydroethidium (DHE) and TRIzol Reagent were from Life Technologies (Carlsbad, CA). Utilized antibodies were obtained from the following sources: mouse monoclonal antibody against LXRα (ab41902) and rabbit polyclonal antibody against LXRβ (ab28479) were from Abcam (Cambridge, UK); rabbit anti-mouse nitrotyrosine antibody (06-284) was from Millipore (Billerica, MA); mouse anti-α-actin antibody (Clone 5C5, A2172) was from Sigma-Aldrich; rabbit anti-caspase-12 (#2202), mouse anti-caspase-9 (C9, #9508), mouse anti-CCAAT/enhancer-binding protein homologous protein (CHOP, L63F7, #2895), rabbit anti-cytochrome *c* (#4272), rabbit anti-voltage-dependent anion channel (VDAC, #4866), and rabbit anti-GAPDH (14C10, #2118) were from Cell Signaling Technology (Beverly, MA); Alexa Fluor® 555 goat anti-mouse IgG antibody (A21422) and Alexa Fluor® 488 goat anti-rat IgG antibody (A-11006) were from Life Technologies; IRDye 800CW goat anti-mouse (926-32210) and anti-rabbit IgG (926-32211) secondary antibodies were from LI-COR Biosciences (Lincoln, NE).

Animals and In-Vivo Experimental Protocols

This investigation conforms to the National Institutes of Health Guidelines on the Use of Laboratory Animals, and was approved by the Institute's Animal Ethics Committee. LXRα-deficient, LXRβ-deficient, LXRα/β-deficient, and wild-type (WT) C57BL/6 male mice (22-25 g) were obtained from the Jackson Laboratories (Bar Harbor, ME), and were housed at 25±5°C, adherent to a 12 hour light-dark cycle. For the acute myocardial ischemia/reperfusion (MI/R) protocol, reperfusion commenced

for 24 hours following 30 minutes of ischemia, and mice were randomly assigned to the following groups: sham, vehicle, 22(*R*)-HC (20 mg/kg), or GW3965 (20 mg/kg) by intraperitoneal injection 15 minutes before reperfusion. Pharmacologic dosages were chosen based upon our pilot study data and the published literature.[1-3] LXRα/β dual agonists at these doses effectively invoked LXR activity without inducing observable hemodynamic changes during in-vivo animal studies.[1-3] To observe the long-term cardioprotective effect of LXRα/β dual agonists, mice were randomly assigned to the following groups: sham, vehicle, 22(*R*)-HC (20 mg/kg), or GW3965 (20 mg/kg) by intraperitoneal injection 15 minutes before reperfusion, and daily following reperfusion for 4 weeks. Other experiments were designed for MI/R outcome determination in LXRα-, β-, and α/β double-deficiency mice and their WT littermates.

Surgical Generation of MI/R Model

MI/R procedures were performed utilizing a novel method as described in our previous studies.[4-7] In brief, the heart was manually exposed without intubation via a small thoracic incision, and a slipknot was tied around the left anterior descending coronary artery 2-3 mm from its origin with a 6-0 silk suture. Sham-operated animals were subjected to identical surgical procedures, except that the suture passed beneath the left anterior descending coronary artery was not tied. After 30 minutes of ischemia, the slipknot was released, and myocardial reperfusion commenced. After recovery from surgery, mice were returned to standard animal housing conditions. Surgical mortality of this MI method is very low (<6%), and no difference was observed between any groups investigated.

In-Vivo siRNA-Mediated Cardiac-Specific Gene Silencing

In-vivo knockdown of cardiac-specific LXRα or LXRβ expression was achieved by intramyocardial delivery of siRNA.[8] FlexiTube HP GenomeWide siRNA targeting mouse LXRα (4 siRNAs in FlexiTube Gene Solution for Mm_Nr1h3; Cat. No.SI00208355, SI02692942, SI02715601, and SI02740339) and LXRβ (4 siRNAs in FlexiTube Gene Solution for Mm_Nr1h2; Cat. No. SI00185227,

SI00185234, SI00185241, and SI02735439) were purchased from Qiagen (Hilden, Germany). AllStars Negative Control siRNA (Qiagen, Cat. No. 1027280) served as negative control. This non-silencing control has no homology to any known mammalian gene, and has been validated using Affymetrix GeneChips (Qiagen). FlexiTube LXRα siRNAs, FlexiTube LXRβ siRNAs, or AllStars Negative Control siRNA were complexed with in-vivo Jet-PEI Delivery Reagent (Polyplus-transfection, Illkirch, France) in 5% glucose per manufacturer's recommendations. Mice were anesthetized with 2% isoflurane, and the heart was exposed via left thoracotomy at the fifth intercostal space. Mouse-specific LXR siRNA or negative control (20 μl; 1 μg/g) was delivered via three separate intramyocardial injections (32.5-gauge needle), temporarily blanching the left ventricular free wall. Our pilot experiments demonstrated cardiac LXR expression reached nadir (~25-30% of control levels) 48 hours after siRNA injection. MI/R protocol was therefore performed 48 hours after intramyocardial siRNA delivery.

In-Vivo Adenoviral-Mediated Cardiac Gene Overexpression

The adenoviral-mediated gene delivery was as previously described.[9] Ad.LXRα, Ad.LXRβ (adenoviruses containing the LXRα or β gene) and Ad.LacZ (negative control) were generated following the instructions of ViraPower Adenoviral Expression System (Life Technologies) per manufacturer protocol. The full-length cDNAs for LXRα or LXRβ was cloned into the pENTR1A vector (Life Technologies) and transferred into the pAd/CMV/V5-DEST vector (Life Technologies) via Gateway LR Clonase II enzyme mix per manufacturer protocol (Life Technologies). The viral titer was determined via Adeno-X Rapid Titer Kit (Clontech Laboratories, Mountain View, CA).The mice were anesthetized with 2% isoflurane, and the heart was exposed via a left thoracotomy at the fifth intercostal space. Adenovirus (5×10^9 IFU/ml) was administered by direct injection into the left ventricular free wall (three sites, 10 μl/site, 32.5-gauge needle). Three days after adenoviral injection, the mice were subjected to coronary artery occlusion and reperfusion as described above. Myocardial LXR expression was analyzed before the MI/R procedures.

Hemodynamic measurements

Blood pressure and heart rate in conscious mice were measured by a tail-cuff system (BP-2010, Softron, Tokyo, Japan), as described previously.[10] Before study initiation, the animals were adapted to the apparatus for at least 5 days. Multiple measurements generated an average value for each animal, and the mean results of each group were calculated from average values.

Western Blot Analysis

Proteins were prepared per standard protocol, and protein lysate concentrations were determined via Pierce BCA Protein Assay Kit (Thermo Scientific, Rockford, IL). To prepare the mitochondrial or cytosolic fractions, protein lysate was collected via Mitochondria Isolation Kit (Thermo Scientific). Equal quantities of proteins (30-50 μg/lane) were submitted to 10 or 12% SDS-PAGE, dependent upon the target proteins, electrotransferred onto nitrocellulose membranes, and incubated with primary antibodies against LXRα (1:1000), LXRβ (1:1000), caspase-12 (1:1000), CHOP (1:1000), caspase-9 (1:1000), and cytochrome *c* (1:1000). GAPDH and VDAC levels were utilized as loading controls for total and mitochondrial protein expression, respectively. After incubation with the corresponding second antibodies, protein bands were detected by an Odyssey® IR scanner (LI-COR Biosciences, Lincoln, NE). Quantitation was performed via Quantity One 4.4.0 software (Bio-Rad, Hercules, CA).

Real-Time Quantitative PCR

Total RNA was isolated from tissues and cardiomyocytes with TRIzol Reagent and purified with Qiagen's RNeasy Mini Kit (Qiagen). Reverse transcription was performed by Omniscript RT Kit (Qiagen). The resultant cDNA was amplified by SYBR® Premix Ex Taq™ Perfect Real Time Kit (Takara BIO, Otsu, Japan). The PCR reaction was directly monitored by The LightCycler® 480 Real-Time PCR System (Roche Applied Science, Indianapolis, IN). Utilized SYBR Green real-time PCR

primers were as follows: mouse LXRα (GenBank Accession No. NM001177730 and NM013839), forward 5'-GCTCATTGCCATCAGCATC–3' and reverse 5'-AGCATCCGTGGGAACATCA-3'; mouse LXRβ (GenBank Accession No. NM009473 and XM_001002072), forward 5'-TGCCAGGGTTCTTGCAGTTG-3' and reverse 5'-AACGTGATGCATTCTGTCTCGTG-3'; mouse NADPH oxidase gp^{91phox} subunit (GenBank Accession No. NM_007807.4), forward 5'-TGATCCTGCTGCCAGTGTGTC-3' and reverse 5'-GTGAGGTTCCTGTCCAGTTGTCTTC-3'; mouse inducible nitric oxide synthase (iNOS) (GenBank Accession No. NM_010927.3), forward 5'-CAAGCTGAACTTGAGCGAGGA-3' and reverse 5'-TTTACTCAGTGCCAGAAGCTGGA-3'; mouse GAPDH (GenBank Accession No. BC083149), forward 5'- TGGCACAGTCAAGGCTGAGA-3' and reverse 5'-CTTCTGAGTGGCAGTGATGG-3'. Real-time PCR data were represented as Ct values, defined as the crossing threshold of PCR, obtained via LightCycler 480 Data Analysis software. Relative mRNA levels of the sample mRNA expression were calculated asdescribed, and expressed as $2^{-\Delta\Delta Ct}$.[4]

In-situ Detection of Apoptosis in Heart Tissue

Myocardial apoptosis was determined by terminal deoxynucleotidyl transferase dUTP nick-end labeling (TUNEL) technique via a Fluorescein In Situ Cell Death Detection Kit (Roche Diagnostics) as described previously.[4, 6, 7] Apoptotic nuclei were detected by green fluorescein staining, cardiomyocytes were identified by anti-α-actin antibody, and total cardiomyocyte nuclei were DAPI labeled.[4] A commercial kit (Roche Diagnostics) was utilized for immunohistochemical detection and quantification of apoptosis (brown staining nuclei).[11] Results were expressed as the percentage of apoptotic cells among the total cell population.

Detection of Caspase Activities in Heart Tissue

Cardiac caspase-3 activity was measured via caspase-3 Colorimetric Assay Kit (Millipore) as previously described.[4, 6, 7] Briefly, 100 μg of total protein from tissues was loaded and incubated with

25 μg Ac-DEVD-pNA (a colorimetric-specific substrate) at 37°C for 1.5 hours. pNA cleaved from DEVD by caspase-3 was quantified by a microplate reader (BioTek, Winooski, VT) at 405 nm. Changes in caspase activity in the MI/R tissue samples were calculated against the mean value of caspase activity from sham experiment tissue, and expressed as pmol pNA/mg protein. Cardiac activation of caspase-8, caspase-9, and caspase-12 was evaluated utilizing respective caspase Fluorometric Assay Kits (BioVision, Mountain View, CA). Briefly, 100 μg of total protein from tissues per assay and a final concentration of 50 μM of AFC-conjugated with substrates specific for caspase-8, -9, and -12 (IEDT, LEHD, and ATAD) respectively was loaded. Samples were read by a fluorimeter equipped with a 400-nm excitation and a 505-nm emission filter. The activities of caspase-8, -9, and -12 were compared to sham control.

Determination of Myocardial Infarct Size

Myocardial infarct size was determined by Evans blue-TTC double staining methods as previously described.[4-7] Briefly, the ligature around the coronary artery was re-tied after reperfusion, and 0.2 ml 2% Evans blue dye was injected into the left ventricular cavity. The dye was circulated and uniformly distributed, except in the cardiac regions previously perfused by the occluded coronary artery area-at-risk (AAR). The heart was quickly excised, frozen at -20°C, and sliced into 1 mm thick sections perpendicular to the long axis of the heart. Slices were incubated individually using a 24-well culture plate in 1% TTC solution (pH 7.4) at 37°C for 10 minutes, and photographed digitally. The Evan's blue-stained area (area not at risk, ANAR), TTC-stained area, and TTC-negative staining area (infarcted myocardium) were measured via computer-based image analyzer SigmaScan Pro 5.0 (Systat Software, Chicago, IL). Myocardial infarct size was expressed as a percentage of the infarct area (I) over AAR (I/AAR); AAR size was expressed as the percentage of AAR over total left ventricular area (AAR/AAR+ANAR), as previously described.[4-7] The myocardial infarct size was expressed as a percentage of infarct area over AAR.

Echocardiographic Measurements

In-vivo cardiac function was determined by echocardiography 24 hours and 4 weeks after reperfusion.[4-7] Mice were anesthetized with 1.5% isoflurane. Two-dimensional echocardiographic views of the mid-ventricular short axis were obtained at the level of the papillary muscle tips below the mitral valve (Vevo 770, VisualSonic, Toronto, Canada). Left ventricular fractional shortening (LVFS) and left ventricular ejection fraction (LVEF) were calculated as previously described.[4-7]

Fluorodeoxyglucose (18F) Micro-Positron Emission Tomography/Computed Tomography (^{18}F-FDG Micro-PET/CT) Scanning and Analysis

Detection of viable myocardium was performed via micro-PET/CT scanning as previously described.[12, 13] The animals were anesthetized with 2% isoflurane in O_2 gas, and received ^{18}F-FDG injection (0.1 ml, single intravenous tail vein injection with activity of 10 MBq[13]). Immediately awakened after injection, the animals were returned to the anesthesia cage. Two hours after administration of the tracer injection, animals were anesthetized with isoflurane, placed prone on the PET/CT scanner bed near the central field of view, and received continuous anesthesia for the study duration. Inveon Acquisition Workplace (IAW) was utilized for the scanning process. Ten-minute static PET scans were acquired and images were reconstructed by a 3-Dimensional Ordered Subsets Expectation Maximum (OSEM3D) algorithm followed by MAP (Maximization/Maximum a Posteriori) or FastMAP provided by IAW. The 3 Dimensional Regions of Interest (3D ROIs) were drawn over the heart guided by CT images and tracer uptake was measured by Inveon Research Workplace (IRW) 3.0 software. Individual quantification of ^{18}F-FDG uptake in each animal was calculated. Mean standardized uptake values (SUV) were determined by dividing the relevant ROI activity by the ratio of the injected dose to body weight as follows:

$$\text{SUV} = \text{ROI activity (MBq/g)} / [\text{injected dose (MBq)}/\text{body weight (g)}]$$

Measurement of Oxidative Stress Generation in Heart Tissue

Myocardial reactive oxygen species generation was measured by confocal microscope via in-situ DHE stain or lucigenin-enhanced chemiluminescence. For DHE stain, unfixed frozen cross-sections (5 μm) were incubated with DHE (5 μmol/L) at 37°C for 30 minutes in a humidified chamber protected from light, followed by 5 minutes of PBS washing to remove nonintercalated ethidium bromide molecules. Images were obtained and analyzed via Leica laser scanning confocal microscope (Leica TCS SP5 II). NADPH oxidase activity within the heart homogenates was measured by lucigenin-enhanced chemiluminescence via luminometer, as previously described.[6, 7] The lucigenin concentration in the final reaction mixture was 0.25 mmol/L, and NADPH-dependent superoxide production was expressed as relative light units (RLU) per mg per second (RLU • mg^{-1} • s^{-1}).

Determination of Nitrative Stress Generation in Heart Tissue

Myocardial nitrative stress was assessed by nitrotyrosine content, a footprint of in-vivo peroxynitrite formation,[6, 7] by both immunostaining and ELISA analysis. For immunostaining, paraffin-embedded slices were stained with primary antibody against nitrotyrosine (1:100), and then immunostained by Vectastain ABC kit (Vector Laboratories, Burlingame, CA; 1:200). For ELISA, cardiac tissue nitrotyrosine content wasquantified by nitrotyrosine ELISA Kit (Abnova, Taiwan). Results were presented as nanomoles/g protein.

Analyses of Lipid Profiles in Heart Tissue

Analyses of lipid profiles was performed via an Agilent 6890 gas chromatography instrument (Santa Clara, CA) with electron Ionization detection as previously described. [14, 15]

Supplemental Results

LXRα activation alters fatty acid profiles in heart tissue in murine MI/R model.

It has been reported that LXR activation in heart leads to alteration of fatty acid composition in favor of accumulation of monosaturates. We thus further investigated the effect of LXR activation on the fatty acid profiles in our MI/R murine models. As shown in the Supplementary Table 1, treatment of GW3965 caused a shift in cardiac fatty acid composition in favor of unsaturates in heart tissue in WT mice, as evidenced by increased ratio of unsaturated fatty acid (including 16:1n9, 16:1n7, 18:1n7 and 20:3n6) and decreased saturated fatty acid (including 16:0 and 18:0). These effects were impaired in LXRα or LXRα/β double KO mice, but not in LXRβ KO mice. Thus, activation of LXRα, but not LXRβ, altered the type of fatty acids in favor of unsaturates.

Supplementary Table 1: Effects of LXR agonist GW3965 on triglyceride fatty acid profile in the ventricles of WT and LXRs KO mice.

Fatty Acid	WT (24h)	WT + GW (24h)	WT (4 weeks)	WT + GW (4 weeks)	LXRα KO (24h)	LXRα KO + GW (24h)	LXRβ KO (24h)	LXRβ KO + GW (24h)	LXRα/β KO (24h)	LXRα/β KO + GW (24h)
14:0	0.1 ± 0.01	0.2 ± 0.006*	0.05 ± 0.02	0.2 ± 0.01†	0.2 ± 0.06	0.2 ± 0.004	0.1 ± 0.02	0.2 ± 0.03	0.2 ± 0.03	0.1 ± 0.02
16:0	14.2 ± 0.9	13.3 ± 0.3	16.3 ± 0.5	14.7 ± 0.2†	13.8 ± 0.8	13.6 ± 0.2	14.1 ± 0.1	14.4 ± 0.4	16.4 ± 0.6	16.9 ± 0.9
16:1n9	0.2 ± 0.01	0.2 ± 0.02	0.1 ± 0.005	0.2 ± 0.01†	0.2 ± 0.04	0.2 ± 0.04	0.06 ± 0.002	0.08 ± 0.008	0.1 ± 0.02	0.1 ± 0.01
16:1n7	0.2 ± 0.02	0.4 ± 0.05*	0.2 ± 0.009	0.5 ± 0.02†	0.6 ± 0.2	0.3 ± 0.05	0.2 ± 0.02	0.3 ± 0.03‡	0.2 ± 0.02	0.2 ± 0.03
18:0	17.6 ± 1.2	16.0 ± 0.5	20.7 ± 1.2	16.4 ± 0.3†	18.3 ± 3.4	16.3 ± 0.6	18.2 ± 0.3	19.4 ± 0.6	20.4 ± 1.2	19.3 ± 1.3
18:1n9	8.9 ± 0.3	10.3 ± 0.7	7.6 ± 0.2	8.7 ± 0.4	12.4 ± 1.8	9.2 ± 0.9	6.4 ± 0.3	5.8 ± 0.4	9.0 ± 0.8	9.1 ± 0.8
18:1n7	2.1 ± 0.09	2.0 ± 0.07	1.9 ± 0.06	2.7 ± 0.03†	2.0 ± 0.08	2.0 ± 0.05	1.9 ± 0.1	1.8 ± 0.04	2.2 ± 0.04	2.1 ± 0.07
18:2n6	19.7 ± 0.6	18.6 ± 0.9	17.6 ± 0.4	17.2 ± 0.6	19.1 ± 1.4	20.4 ± 1.1	16.8 ± 0.6	14.1 ± 0.9	18.1 ± 1.3	17.5 ± 1.9
20:0	0.3 ± 0.03	0.3 ± 0.009	0.5 ± 0.03	0.3 ± 0.01†	0.5 ± 0.09	0.3 ± 0.07	0.4 ± 0.01	0.4 ± 0.04	0.4 ± 0.02	0.4 ± 0.04
20:3n6	0.6 ± 0.02	0.8 ± 0.04*	0.5 ± 0.01	0.7 ± 0.02†	0.5 ± 0.04	0.6 ± 0.02	0.5 ± 0.02	0.9 ± 0.07‡	0.5 ± 0.04	0.6 ± 0.06
20:4n6	5.2 ± 0.2	4.9 ± 0.2	5.6 ± 0.1	7.3 ± 0.2	4.1 ± 1.0	6.2 ± 0.3	7.1 ± 0.3	6.9 ± 0.4	6.5 ± 0..3	6.7 ± 0.4
22:5n3	1.4 ± 0.03	1.8 ± 0.04	1.7 ± 0.1	1.8 ± 0.06	1.1 ± 0.2	1.7 ± 0.03	1.7 ± 0.05	1.8 ± 0.1	1.5 ± 0.1	1.6 ± 0.09
22:6n3	29.5 ± 2.1	31.2 ± 1.2	27.3 ± 1.5	29.5 ± 0.7	27.2 ± 2.2	29.1 ± 1.3	32.7 ± 0.8	34.2 ± 1.7	24.5 ± 0.7	25.4 ± 1.8

Values (means ± SEM) represent relative distribution (%) of different fatty acids in the triglyceride fraction isolated from MI/R murine ventricles. For the acute MI/R protocol, reperfusion commenced for 24 hours following 30 minutes of ischemia, and mice were randomly assigned to receive GW3965 (20 mg/kg) or vehicle 15 minutes before reperfusion. To observe the long-term cardioprotective effect of LXR activation, mice were randomly assigned to receive GW3965 (20 mg/kg) or vehicle 15 minutes before reperfusion, and daily following reperfusion for 4 weeks [n = 6-10 in each group; *P<0.05 vs. WT (24h) group, †P< 0.05 vs. WT (4 weeks) group, ‡P< 0.05 vs. LXRβ KO (24h) group]. Abbreviations: MI/R, myocardial ischemia/reperfusion; WT, wild type; KO, knockout; GW, GW3965.

Supplemental Figures and Figure Legends

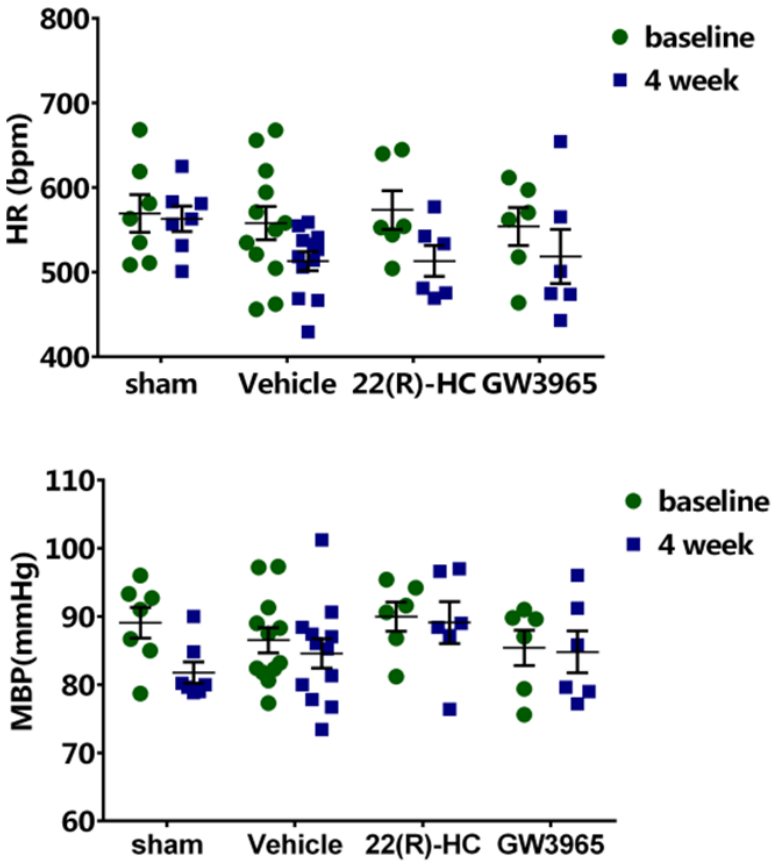

Figure S1. LXRα/β dual agonists induced no observable hemodynamic changes in myocardial ischemia/reperfusion (MI/R) models.

Changes in heart rate and mean arterial pressure in each group (n=6-12) during the experiment. Abbreviations: 22(*R*)-HC, 22(*R*)-hydroxycholesterol; HR, heart rate; MBP, mean arterial blood pressure.

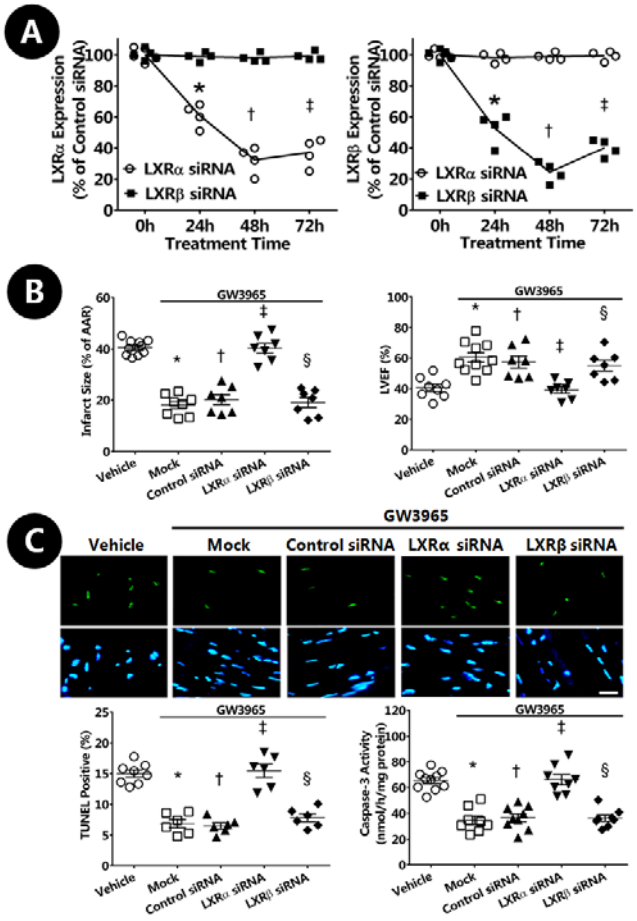

Figure S2. Cardioprotective effects of LXRα/β dual agonist were lost in cardiac-specific LXRα–knockdown (KD) mice. A. Intramyocardial delivery of siRNA against LXRα or LXRβ effectively eliminated the expression of LXRα or LXRβ, respectively, in left ventricle. Time-courses changes in LXRα or LXRβ expression by real-time PCR after siRNA delivery are shown. Results were expressed as percentages of the control siRNA (n=4-5; LXRα: *P=0.55, †P=0.003, ‡P=0.01 vs. the control siRNA group; LXRβ: *P=0.39, †P=0.0007, ‡P=0.060 vs. the control siRNA group). **B-C.** Effect of cardiac-specific-KD of LXRα or LXRβ by in-vivo siRNA transfection upon MI/R injury. MI/R procedures were performed 48 hours after intramyocardial siRNA delivery. GW3965 (20mg/kg) was administered 15 minutes before reperfusion. **B.** MI/R injury was assessed by myocardial infarction size as determined by Evans blue/TTC double-staining (n=7-10; *P=0.0004, †P=0.006, ‡P>0.99, §P=0.002 vs. vehicle), and left ventricular dysfunction was determined by echocardiography (n=7-10; *P=0.002, †P=0.02, ‡P>0.99, §P=0.048 vs. vehicle). **C.** Myocardial apoptosis was determined by TUNEL labeling (n=6-8; Bar=25 μm; *P=0.006, †P=0.002, ‡P>0.99, §P=0.04 vs. vehicle) and caspase-3 activation (n=8-10; *P=0.0004, †P=0.002, ‡P>0.99, §P=0.002 vs. vehicle). Abbreviations: MI/R, myocardial ischemia/reperfusion; AAR, area at risk; LVEF, left ventricular ejection fraction; TUNEL, terminal deoxynucleotidyl transferase dUTP nick end labeling.

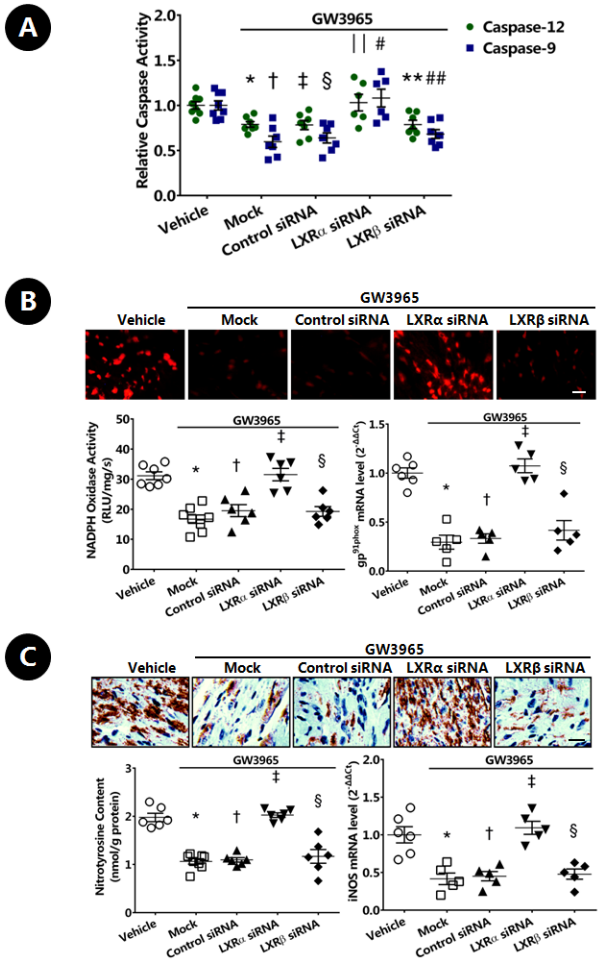

Figure S3. Anti-oxidative/nitrative and anti-apoptosis effects of LXRα/β dual agonist were lost in LXRα-knockdown (KD) mice. A-C. Effect of LXRα or LXRβ gene KD upon MI/R injury. GW3965 (20mg/kg) was injected 15 minutes before reperfusion. **A.** Caspase-9 and caspase-12 activity was measured by fluorometric assay (n=6-8; caspase-12: *P=0.03, ‡P=0.04, ||P>0.99, **P=0.04 vs. vehicle; caspase-9: †P=0.004, §P=0.01, #P>0.99, ##P=0.04 vs. vehicle). **B.** Myocardial oxidative stress was measured utilizing confocal microscope with in-situ dihydroethidium stain (n=5-6; Bar=25 μm), NADPH oxidase activity by lucigenin-enhanced chemiluminescence (n=6-8; *P=0.001, †P=0.03, ‡P>0.99, §P=0.03 vs. vehicle), and NADPH oxidase gp^{91phox} gene expression by real-time PCR (n=5-6; *P=0.009, †P=0.04, ‡P>0.99, §P=0.05 vs. vehicle). Results were normalized against GAPDH and converted to fold induction relative to vehicle group. **C.** Myocardial nitrative stress was assessed by nitrotyrosine content determined by immunohistochemistry (n=5-6; Bar=25 μm) and ELISA assay (n=6-8; *P=0.007, †P=0.01, ‡P>0.99, §P=0.04 vs. vehicle). The gene expression of iNOS was determined by real-time PCR (n=5-6; *P=0.02, †P=0.03, ‡P>0.99, §P=0.048 vs. vehicle). Results were normalized against GAPDH and converted to fold induction relative to vehicle group. Abbreviations: MI/R, myocardial ischemia/reperfusion; RLU, relative light units; iNOS, inducible nitric oxide synthase.

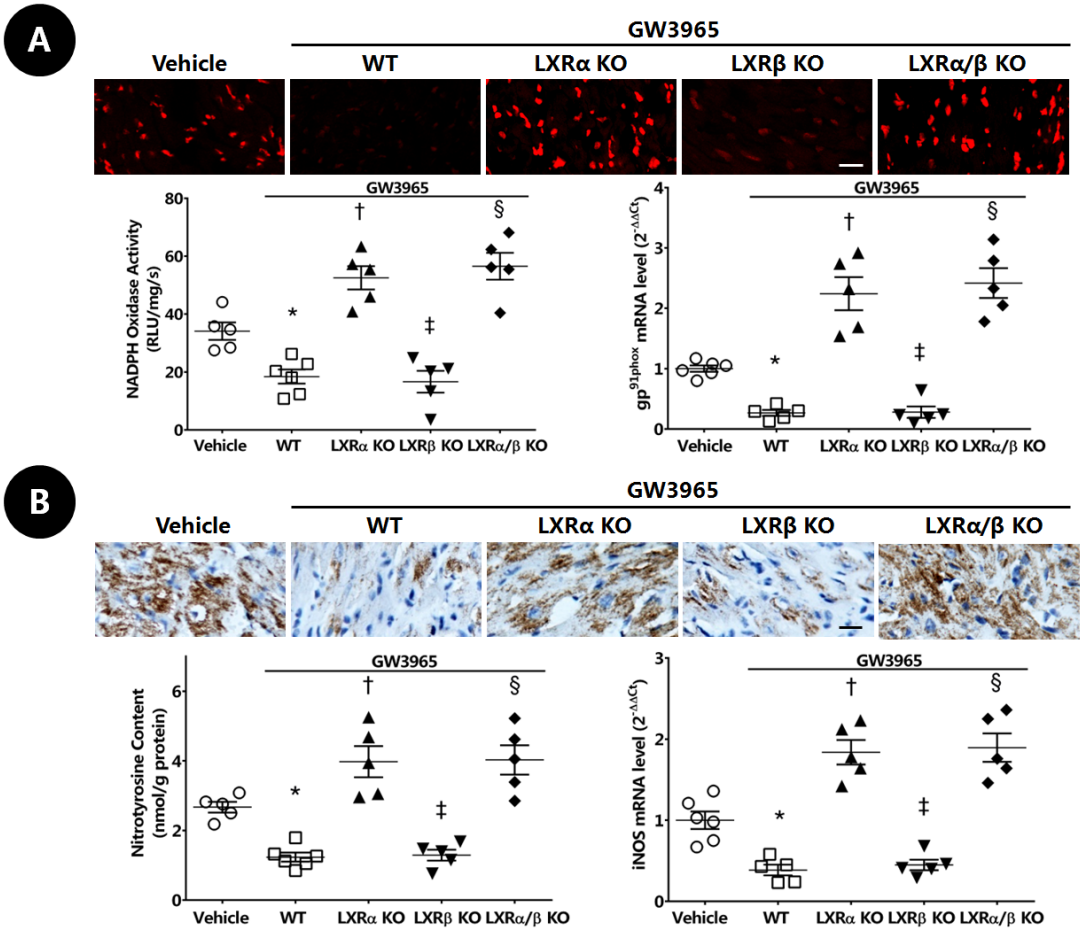

Figure S4. Anti-oxidative and anti-nitrative effects of LXRα/β dual agonist were lost in LXRα/β double- and LXRα-knockout (KO) mice. A. Myocardial oxidative stress was measured utilizing confocal microscope with in-situ dihydroethidium stain (n=5-6 hearts per group, Bar=25 μm). NADPH oxidase activity was assessed by lucigenin-enhanced chemiluminescence (n=5-6; *P=0.01, †P=0.047, ‡P=0.01, §P=0.02 vs. vehicle). NADPH oxidase gp^{91phox} gene expression was determined by real-time PCR (n=5-6; *P=0.02, †P=0.02, ‡P=0.006, §P=0.005 vs. vehicle). Results were normalized against GAPDH and converted to fold induction relative to vehicle group. **B.** Myocardial nitrative stress was assessed by nitrotyrosine content determined by immunohistochemistry (n=5-6 hearts per group, Bar=25 μm) and ELISA assay (n=5-6; *P=0.006, †P=0.04 ‡P=0.03, §P=0.04 vs. vehicle). The gene expression of iNOS was determined by real-time PCR (n=5-6; *P=0.008, †P=0.02, ‡P=0.03, §P=0.007 vs. vehicle). Results were normalized against GAPDH and converted to fold induction relative to vehicle group. Abbreviations: WT, wild type; RLU, relative light units; iNOS, inducible nitric oxide synthase.

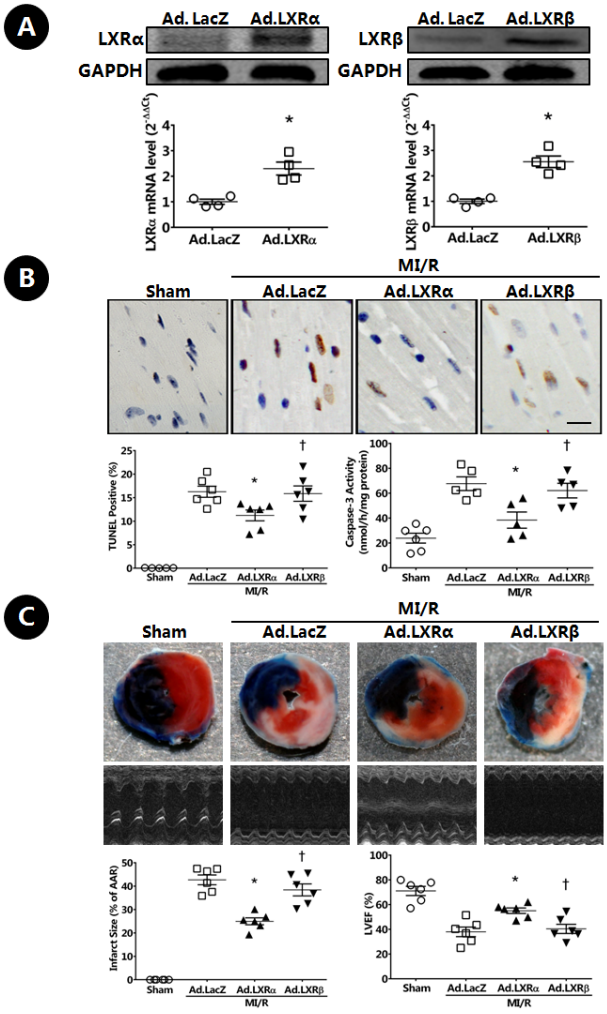

Figure S5. Cardiac LXRα overexpression inhibited MI/R-induced myocardial apoptosis, infarct size, and cardiac dysfunction. A. Cardiac LXRα and LXRβ alteration after adenovirus-mediated cardiac-specific gene delivery. LXR protein and gene alteration detected by Western blot and real-time quantitative PCR from mouse left ventricular tissues. Adenovirus-encoded LacZ (Ad.LacZ) treatment served as control. Results were normalized against GAPDH and converted to fold induction relative to Ad.LacZ group (n=4; LXRα: *P=0.03 vs. Ad.LacZ; LXRβ: *P =0.03 vs. Ad.LacZ). **B-C.** Effect of LXRα or LXRβ gene overexpression upon MI/R injury. **B.** Myocardial apoptosis was determined by immunohistochemical staining of TUNEL (n=5-6, Bar=25 μm; *P=0.04, †P>0.99, vs. Ad.LacZ) and caspase-3 activation (n=5-6; *P=0.03, †P>0.99, vs. Ad.LacZ). **C.** MI/R injury was assessed by myocardial infarction size as determined by Evans blue/TTC double-staining (n=6; *P=0.001, †P=0.66, vs. Ad.LacZ), and left ventricular dysfunction was determined by echocardiography (n=6; *P=0.02, †P>0.99, vs. Ad.LacZ). Abbreviations: Ad., adenoviral-encoded; MI/R, myocardial ischemia/reperfusion; AAR, area at risk; TUNEL, terminal deoxynucleotidyl transferase dUTP nick end labeling; LVEF, left ventricular ejection fraction.

Supplemental References

1. Morales JR, Ballesteros I, Deniz JM, Hurtado O, Vivancos J, Nombela F, Lizasoain I, Castrillo A, Moro MA. Activation of liver X receptors promotes neuroprotection and reduces brain inflammation in experimental stroke. *Circulation.* 2008;118:1450-1459.
2. Leik CE, Carson NL, Hennan JK, Basso MD, Liu QY, Crandall DL, Nambi P. GW3965, a synthetic liver X receptor (LXR) agonist, reduces angiotensin II-mediated pressor responses in Sprague-Dawley rats. *Br J Pharmacol.* 2007;151:450-456.
3. Wang YY, Dahle MK, Steffensen KR, Reinholt FP, Collins JL, Thiemermann C, Aasen AO, Gustafsson JA, Wang JE. Liver X receptor agonist GW3965 dose-dependently regulates lps-mediated liver injury and modulates posttranscriptional TNF-alpha production and p38 mitogen-activated protein kinase activation in liver macrophages. *Shock.* 2009;32:548-553.
4. Pu J, Yuan A, Shan P, Gao E, Wang X, Wang Y, Lau WB, Koch W, Ma XL, He B. Cardiomyocyte-expressed farnesoid-X-receptor is a novel apoptosis mediator and contributes to myocardial ischaemia/reperfusion injury. *Eur Heart J.* 2013;34:1834-1845.
5. Gao E, Lei YH, Shang X, Huang ZM, Zuo L, Boucher M, Fan Q, Chuprun JK, Ma XL, Koch WJ. A novel and efficient model of coronary artery ligation and myocardial infarction in the mouse. *Circ Res.* 2010;107:1445-1453.
6. Wang Y, Gao E, Tao L, Lau WB, Yuan Y, Goldstein BJ, Lopez BL, Christopher TA, Tian R, Koch W, Ma XL. AMP-activated protein kinase deficiency enhances myocardial ischemia/reperfusion injury but has minimal effect on the antioxidant/antinitrative protection of adiponectin. *Circulation.* 2009;119:835-844.
7. Tao L, Gao E, Jiao X, Yuan Y, Li S, Christopher TA, Lopez BL, Koch W, Chan L, Goldstein BJ, Ma XL. Adiponectin cardioprotection after myocardial ischemia/reperfusion involves the reduction of oxidative/nitrative stress. *Circulation.* 2007;115:1408-1416.

8. Wang Y, Lau WB, Gao E, Tao L, Yuan Y, Li R, Wang X, Koch WJ, Ma XL. Cardiomyocyte-derived adiponectin is biologically active in protecting against myocardial ischemia-reperfusion injury. *Am J Physiol Endocrinol Metab.* 2010;298:E663-E670.

9. Ma H, Wang J, Thomas DP, Tong C, Leng L, Wang W, Merk M, Zierow S, Bernhagen J, Ren J, Bucala R, Li J. Impaired macrophage migration inhibitory factor-AMP-activated protein kinase activation and ischemic recovery in the senescent heart. *Circulation.* 2010;122:282-292.

10. Hishikari K, Suzuki J, Ogawa M, Isobe K, Takahashi T, Onishi M, Takayama K, Isobe M. Pharmacological activation of the prostaglandin E2 receptor EP4 improves cardiac function after myocardial ischaemia/reperfusion injury. *Cardiovasc Res.* 2009;81:123-132.

11. Lu D, Lian H, Zhang X, Shao H, Huang L, Qin C, Zhang L. LMNA E82K mutation activates FAS and mitochondrial pathways of apoptosis in heart tissue specific transgenic mice. *PLoS One.* 2010;5:e15167.

12. Eguchi M, Kim YH, Kang KW, Shim CY, Jang Y, Dorval T, Kim KJ, Sweeney G. Ischemia-reperfusion injury leads to distinct temporal cardiac remodeling in normal versus diabetic mice. *PLoS One.* 2008;7:e30450.

13. Laurberg JM, Olsen AK, Hansen SB, Bottcher M, Morrison M, Ricketts SA, Falk E. Imaging of vulnerable atherosclerotic plaques with FDG-microPET: no FDG accumulation. *Atherosclerosis.* 2007;192:275-282.

14. Yi LZ, He J, Liang YZ, Yuan DL, Chau FT. Plasma fatty acid metabolic profiling and biomarkers of type 2 diabetes mellitus based on GC/MS and PLS-LDA. *FEBS Lett*. 2006;580:6837-6845.

15. Lei P, Baysa A, Nebb HI, Valen G, Skomedal T, Osnes JB, Yang Z, Haugen F. Activation of Liver X receptors in the heart leads to accumulation of intracellular lipids and attenuation of ischemia-reperfusion injury. *Basic Res Cardiol*. 2013;108:323.